On the Performance of Serially Concatenated CPM-OFDMA Schemes for Aeronautical Telemetry

A
F
F
T
C

Marilynn Wylie, Glenn Green

**AIR FORCE FLIGHT TEST CENTER
EDWARDS AFB, CA**

4/18/11

**AIR FORCE FLIGHT TEST CENTER
EDWARDS AIR FORCE BASE, CALIFORNIA
AIR FORCE MATERIEL COMMAND
UNITED STATES AIR FORCE**

REPORT DOCUMENTATION PAGE

1. REPORT DATE (DD-MM-YYYY) 18-04-2011	2. REPORT TYPE Technical Paper	3. DATES COVERED (From - To) April11—May11

4. TITLE AND SUBTITLE

On the Performance of Serially Concatenated CPM-OFDMA Schemes for Aeronautical Telemetry

5a. CONTRACT NUMBER

5b. GRANT NUMBER

5c. PROGRAM ELEMENT NUMBER

6. AUTHOR(S)

Marilynn Wylie, Glenn Green

5d. PROJECT NUMBER

5e. TASK NUMBER

5f. WORK UNIT NUMBER

7. PERFORMING ORGANIZATION NAME(S) AND ADDRESS(ES) AND ADDRESS(ES)

Gem Direct, Inc., Irving, TX

8. PERFORMING ORGANIZATION REPORT NUMBER
AFFTC-PA-10971

9. SPONSORING / MONITORING AGENCY NAME(S) AND ADDRESS(ES)
Tom Young

10. SPONSOR/MONITOR'S ACRONYM(S)
N/A

11. SPONSOR/MONITOR'S REPORT NUMBER(S)

12. DISTRIBUTION / AVAILABILITY STATEMENT
Approved for public release A: distribution is unlimited.

13. SUPPLEMENTARY NOTES
CA: Air Force Flight Test Center Edwards AFB CA   CC: 012100

14. ABSTRACT

Abstract—In this paper, we investigate the performance of a serially concatenated CPM-OFDM (Continuous Phase Modulation Orthogonal Frequency Division Multiplexing) scheme in various frequency selective fading environments that are typical for aeronautical telemetry. CPM-OFDM is a novel modulation technique that assigns the sampled, complex outputs of a CPM to a set of orthogonal subcarriers for a DFT-precoded OFDM style transmission. This approach maintains much of the power efficiency of CPM while incorporating the spectral efficiency of OFDM. At the receiver, low complexity frequency domain equalization techniques can be applied to mitigate the impact of the radio channel. Although uncoded CPM-OFDMA has been investigated, coded CPM-OFDMA is a new area of focus, which promises to offer good performance in highly dynamic telemetry environments. The serially concatenated code is comprised of an inner code and an outer code. The inner code is generated from the discrete time samples of a PCM-FM modulation while the outer code is derived from a nonrecursive convolutional code. We evaluate the proposed scheme over the additive white Gaussian noise channel as well as in two frequency selective fading environments that are characteristic of aeronautical telemetry.

15. SUBJECT TERMS
Continuous Phase Modulation Orthogonal Frequency Division Multiplexing, Continuous Phase Modulation, PCM/FM, Spectral Efficiency, CPM-OFDM

16. SECURITY CLASSIFICATION OF: **Unclassified**			17. LIMITATION OF ABSTRACT	18. NUMBER OF PAGES	19a. NAME OF RESPONSIBLE PERSON 412 TENG/EN (Tech Pubs)
a. REPORT Unclassified	b. ABSTRACT Unclassified	c. THIS PAGE Unclassified	None	6	19b. TELEPHONE NUMBER (include area code) 661-277-8615

On the Performance of Serially Concatenated CPM-OFDM Schemes for Aeronautical Telemetry

Marilynn Wylie and Glenn Green [a]

Gem Direct Inc.

Abstract— In this paper, we investigate the performance of a serially concatenated CPM-OFDM (Continuous Phase Modulation Orthogonal Frequency Division Multiplexing) scheme in various frequency selective fading environments that are typical for aeronautical telemetry.

CPM-OFDM is a novel modulation technique that assigns the sampled, complex outputs of a CPM to a set of orthogonal subcarriers for a DFT-precoded OFDM style transmission. This approach maintains much of the power efficiency of CPM while incorporating the spectral efficiency of OFDM. At the receiver, low complexity frequency domain equalization techniques can be applied to mitigate the impact of the radio channel.

Although uncoded CPM-OFDMA has been investigated, coded CPM-OFDMA is a new area of focus, which promises to offer good performance in highly dynamic telemetry environments. The serially concatenated code is comprised of an inner code and an outer code. The inner code is generated from the discrete-time samples of a PCM-FM modulation while the outer code is derived from a nonrecursive convolutional code. We evaluate the proposed scheme over the additive white Gaussian noise channel as well as in two frequency selective fading environments that are characteristic of aeronautical telemetry.

I. Introduction

CONTINUOUS phase modulation (CPM) forms a class of constant envelope, continuous phase signaling formats that are known to be efficient in both power and bandwidth [1]. The constant envelope property results in a peak-to-average power ratio of unity, thus making it ideal in aeronautical telemetry applications, where restrictions on device size and weight warrant efficient power amplification.

Advances in modern telemetry system complexity have driven operation to larger bands in order to accommodate data rates on the order of 10-20 Mbits/s in the spectrum allocated to aeronautical telemetry in the United States. Consequently, spectral efficiency has become an important criterion for system design and performance.

While PCM/FM has been the dominant form of carrier modulation in aeronautical telemetry for over 40 years, it lacks the spectral efficiency of other continuous phase modulations that are also used for telemetry – such as shaped offset QPSK (SOQPSK-TG) [2], the Feher patented QPSK (FQPSK) [3] and the Advanced Range Telemetry (ARTM) multi-h CPM Tier II waveform [4].

In this paper, we describe a spectrally efficient implementation of PCM-FM that is based on the use of CPM-OFDM. CPM-OFDM is a modulation scheme that combines power efficient CPM with spectrally efficient OFDM. The implements the discrete-time equivalent of a continuous phase modulator. Those samples are then DFT-spread and mapped to the available subcarriers for an OFDM style transmission. Thus, the contribution of the CPM is to create a serial stream of constant-envelope symbols that maintain the high power efficiency of CPM. Use of OFDM enhances the spectral efficiency and facilitates the use of low complexity equalization techniques at the receiver.

Other approaches to combining CPM with OFDM have been reported, and we briefly discuss some of those results here. An alternate approach involves the transformation of OFDM signals into constant envelope waveforms by *phase modulating* the OFDM waveform. In [5], an OFDM waveform is used to phase modulate a single carrier, and the result is a constant-envelope waveform (i.e., the resulting signal has 0 dB PAPR). In [6], a similar approach is taken whereby the encoded data is first applied to a DCT (discrete cosine transform) and then passed through a continuous phase modulation (CPM) unit. Although both approaches are novel and result in a constant envelope waveform, neither approach retains the orthogonality of the subcarriers. This implies that some of the advantages of using OFDM—such as low complexity frequency domain equalization and frequency multiplexing of user data on the uplink—are lost.

In this study, we focus on PCM-FM as the underlying CPM modulation for the CPM-OFDM waveform, and we demonstrate that good performance can be obtained by sampling the PCM-FM only *once* per symbol interval. This is the most spectrally efficient implementation of PCM-FM/CPM-OFDM. In addition, we also investigate the receiver performance of serially concatenated convolutionally encoded PCM-FM/CPM-OFDM in several frequency selective fading channel environments. Different coding rates are investigated, particularly higher rate codes, as spectral efficiency remains a key concern during telemetry testing and evaluation excercises. Our simulation results show that good bit error rate performance can be obtained by the use of low complexity frequency domain equalization techniques at the receiver, just as in OFDM.

The rest of this paper is organized as follows. Section II gives a brief discussion of the CPM-OFDM signal model. In Section III, we discuss serially concated convolutionally encoded CPM-OFDM. The groundwork for performing low complexity frequency domain equalization is shown in Section IV. V contains a describption of the frequency selective fading channel models used in this study. Finally, in Section VII, we analyze the outcome of our simulation studies.

II. CPM-OFDM Signal Model

In CPM-OFDM, an underlying CPM is sampled N_s times per symbol interval, and the output is treated as a serial stream of encoded symbols. The symbols are then mapped to the frequency domain via the DFT (Discrete Fourier Transform) operation, and the DFT coefficients are mapped to the available set of subcarriers for an OFDM style of transmission. In this paper, we consider the most spectrally efficient case ($N_s = 1$), which corresponds to one sample per CPM symbol interval. This selection minimizes the number of subcarriers used to convey information through the radio channel.

Over the OFDM symbol period, T, a complex-baseband CPM-OFDM signal has the following representation

$$s(t) = \sum_{k=0}^{N-1} S_k(\beta) e^{j2\pi kt/T} \quad 0 \le t < T \quad (1)$$

where the data symbols $S_k(\boldsymbol{\beta})$ are the DFT coefficients of a constant envelope encoder, $s_n(\boldsymbol{\beta})$. The DFT transformation

$$S_k(\boldsymbol{\beta}) = \frac{1}{N} \sum_{n=0}^{N-1} s_n(\boldsymbol{\beta}) e^{j2\pi kn/N} \quad (2)$$

maps the output of the constant envelope encoder

$$s_n(\boldsymbol{\beta}) = e^{j\phi_n(\boldsymbol{\beta})} \quad (3)$$

to the frequency domain. The encoder phase is of the form

$$\phi_n(\boldsymbol{\beta}) = 2\pi h \sum_{i=n-(L-1)}^{n} \beta_i q_{n-i} + \pi h \sum_{i=0}^{n-L} \beta_i. \quad (4)$$

$\beta_i \in \{\pm 1, \pm 3, \cdots, \pm(M-1)\}$ is the ith M-ary (possibly coded) symbol and h is the (rational) digital modulation index.

The phase response q_n is defined as the sampled output of a continuous time-integral of a frequency pulse $F(t)$ with area $1/2$, i.e.

$$q_n = \begin{cases} 0 & n < 0 \\ \int_0^{nT_s} F(\lambda) \, d\lambda & 0 \le n < L \\ \frac{1}{2} & n \ge L \end{cases} \quad (5)$$

where the integer L denotes the pulse duration, expressed in symbol durations, T_s.

The second term on the right hand side of (4) is called the cumulative phase and represents the contribution to the carrier phase from all symbols that have worked their way through the time-varying portion of the phase response and thus contribute a constant value to the overall phase. Since the modulation index h is a rational number, it is drawn from a finite alphabet. In this case, the CPM-OFDM signal can be described as a finite state machine, with a corresponding trellis diagram, and a maximum likelihood sequence detection (MLSD) scheme can be implemented using the Viterbi algorithm (VA) [1].

In this paper, we focus on the implementation of a serially concatenated convolutionally encoded CPM-OFDM that is based upon the manipulation of a PCM-FM waveform.

Since PCM-FM is binary, it follows that $M = 2$. Furthermore, in this case, the frequency pulse is a raised cosine

$$F_{LRC}(t) = \begin{cases} \frac{1}{2LT_s} \left[1 - \cos\left(\frac{2\pi t}{LT_s}\right) \right] & 0 \le t < LT_s \\ 0 & \text{otherwise,} \end{cases} \quad (6)$$
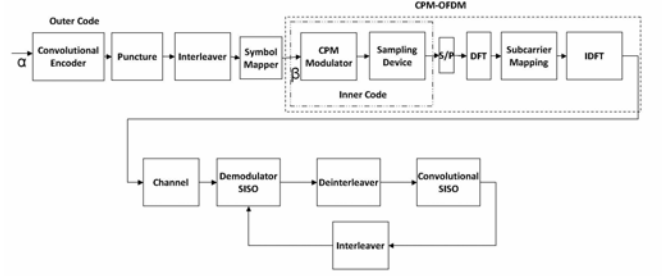

Fig. 1. Serially concatenated convolutional coding with CPM-OFDM.

the signal memory $L = 2$ and the modulation index, $h = 7/10$.

III. Serially Concatenated Convolutionally Encoded CPM-OFDM

In this paper, we focus on a serially concatenated, convolutionally encoded implementation of PCM-FM/CPM-OFDM, where the symbols, β_i are convolutionally encoded and interleaved, as depicted in Fig. (1).

In serially concatenated convolutionally encoded schemes, the outer code is non-recursive while the inner code is recursive. This implementation facilitates the interleaver gain. It can be shown that the samples in (3) can be expressed as the concatenation of two devices: the discrete-time equivalent of a continuous phase encoder and a memoryless discrete-time modulator. Thus, it can be modeled as a rate-1 recursive code. Hence, a coded and interleaved CPM-OFDM can be formed by substituting the discrete-time constant envelope output of the CPM-OFDM for the recursive (inner) convolutional code in a serially concatenated scheme.

In this study, we have investigated a rate $1/2$ convolutional code as the outer code with constraint length $k = 2$ and octal generator $(5, 7)$, which is explained in [7]. This outer encoder is non-recursive with a free distance of $d_{\text{free}} = 5$. The outer code and inner codes are separated by an S-random interleaver.

Since high spectral efficiency is a key concern in telemetry applications, we have investigated the performance of different rate codes by using puncturing. This provides a low complexity method of achieving higher rate codes from the base rate $1/2$ convolutional code. Table specifies the coding rates along with the associated number of input and coded bits for each case under study.

The iterative decoder for serially concatenated convolutionally encoded CPM-OFDM consists of two APP (a posteriori) decoders, one for the inner CPM-OFDM and the other for the outer convolutional code. The demodulators for these codes are based on the soft-input soft-output (SISO) algorithm [11], [12], where the extrinsic information is exchanged between the two decoders for a few iterations before the final estimate of the information symbol sequence is determined. The two SISO modules implement the "max-log" variant of the SISO algorithm. Hence, the soft probabilities are in the form of log-likelihood reatios. The CPM-OFDM SISO demodulator takes the received signal and a soft input on the probability of the coded symbols, $\boldsymbol{\beta}$, and updates the probability of the coded symbols. This output is then deinterleaved and used as a soft

TABLE I
CODING RATES

Coding Rate	Info. Bits (α)	Coded Bits (β)
1/2	1024	2048
2/3	1024	1536
7/8	1022	1168
8/9	1022	1152

input to the convolutional SISO decoder. This outer SISO decoder produces updated versions of its inputs. One output is interleaved and fed back into the CPM-OFDM SISO module. After several iterations, the final output of the convolutional SISO decoder is hard coded to become the final estimate of the information bits, α.

IV. LOW COMPLEXITY FREQUENCY DOMAIN EQUALIZATION

When the CPM-OFDMA signal passes through a frequency-selective channel, the receiver must take the additional step of equalizing the received signal prior to decoding the information bits. This is facilitated at the transmitter side by first adding a cyclic prefix to the post-IDFT sequence by copying the last T_g seconds of the OFDM $v(t)$ to the beginning of the waveform, such that what is transmitted across the channel becomes

$$\tilde{s}(t) = \begin{cases} s(t+T) & -T_g \leq t < 0 \\ s(t) & 0 \leq t < T. \end{cases} \quad (7)$$

After reception, the first T_g samples corresponding to the guard interval (i.e., cyclic prefix) are discarded. The received waveform is sampled and the signal samples that are to be processed can be modeled as

$$r_n = h_n \otimes s_n + w_n \quad (8)$$

where $\otimes$ denotes circular convolution and h_n is the discrete time equivalent of the channel's impulse response.

It is well known that frequency domain equalization (FDE) for cyclic channels can be performed with low computational complexity. We present here a frequency domain equalizer for CPM-OFDM. Assuming that J CPM-OFDM symbols are sent per frame and that there are N_s samples per CPM symbol interval, we can model the DFT of the received (sampled) signal as follows

$$R_k = H_k S_k + W_k, \qquad k = 0, \cdots, JN_s - 1, \quad (9)$$

where H_k denotes the DFT coefficient of the channel impulse response: $(h_n \xrightarrow{\text{DFT}} H_k)$, S_k is the DFT of the signal s_n and W_k is the DFT of the AWGN ($w_n \xrightarrow{\text{DFT}} W_k$).

The frequency response of the MMSE equalizer is given by

$$\hat{H}_k = \frac{H_k^*}{|H_k|^2 + 1/(E_s/N_0)} \quad (10)$$

where E_s/N_0 denotes the symbol energy to noise-PSD ratio. In the frequency domain, the received signal is multiplied by the equalizer coefficients to yield the equalized signal

$$\hat{R}_k = \hat{H}_k R_k, \qquad k = 0, \cdots, JN_s - 1. \quad (11)$$

The equalized signal is then transformed back to the time domain using the IDFT: $\hat{R}_k \xrightarrow{\text{IDFT}} \hat{r}_n$, which is then applied to the Viterbi Algorithm for Maximum Likelihood Sequence Detection.

V. FREQUENCY SELECTIVE FADING CHANNEL MODELS

In this study, we consider CPM-OFDMA performance in a class of wide-band channel models, which feature arrival/take off and parking situations.

Based on a published set of measurement results and empirical data, the models that are expressed in [8] cover a range of telemetry channel models that are suitable for use in channel emulators to validate the performance of schemes that are used for aeronautical links. A detailed discussion of the selected parameter values is provided in [8] for a typical set of aeronautical simulations. A subset of the results are summarized in Table (II).

In the exposition to follow, we offer a brief explanation of the parameters. It is important to note that we have investigated channels and aeronautical scenarios wherein the Doppler is negligible, or zero. [8] actually considers the full range of scenarios (including an en-route scenario wherein the vehicle speeds are expected to be hundreds of m/s).

The time domain representation of the frequency selective fading channel is given by

$$h(\tau, t) = \frac{c}{\sqrt{L_c}} \sum_{n=1}^{L_c} g_n \cdot \frac{\sin(\pi(\tau - \tau_n))}{\pi(\tau - \tau_n)} \quad (12)$$

where g_n denotes a complex Gaussian random variable with mean 0 and unit standard deviation. τ_n indicates the excess path delay. We note that in this model $\tau_n \neq 0 \ \forall n$. L_c denotes the number of taps used to represent the channel.

A Ricean (i.e., nonfading, line of sight) component can be modeled by introducing a constant to the Rayleigh fading process. The complex-valued direct line of sight component is modeled as

$$h_{LOS}(t) = a\delta(t) \quad (13)$$

The parameters a and c are related to the Ricean factor, K_{Rice}, and normalized to conform to the following constraints:

$$a^2 + c^2 = 1 \quad (14)$$

$$a = \sqrt{\frac{K_{Rice}}{K_{Rice} + 1}} \quad (15)$$

$$c = \sqrt{\frac{1}{K_{Rice} + 1}} \quad (16)$$

The first constraint (14) normalizes the channel to have unit power. This implies that the throughput power of the signal remains unchanged due to the presence of the channel. In the limit, as $K_{Rice} \to 0$, this becomes the Rayleigh fading channel, where $a = 0$ and $c = 1$. Conversely, in the limit as $K_{Rice} \to \infty$ (additive white Gaussian noise (AWGN)), one obtains $a = 1$ and $c = 0$, respectively.

In all cases, the values of the delay (τ_n) are obtained using a one-sided exponentially decreasing power delay spectrum, which is defined as

$$\tau_n = -\tau_{slope} \cdot \ln\left(1 - u_n \cdot e^{-\tau_{\max}/\tau_{slope}}\right). \quad (17)$$

TABLE II
SET OF TYPICAL AERONAUTICAL SCENARIOS FOR SIMULATIONS.

	Parking Scenario	Arrival Scenario
Aircraft velocity v [m/s]	$5.5\ (0\cdots5.5)$	$150.0\ (25\cdots150)$
Maximum delay $\tau_{\max}$	$7.0\cdot10^{-6}$	$7.0\cdot10^{-6}$
Number of echo paths	20	20
Rice factor K_{Rice} [dB]	–	$15.0\ (9\cdots20)$
Slope time τ_{slope} [s]	$1.0\cdot10^{-6}$	$1.0\cdots10^{-6}$

u_n denotes a random variable that is uniformly distributed over the interval $u_n \in (0,1)$.

Based on measurements, two different scenarios that are relevant to aeronautical communication, are investigated in this study. These are the parking and arrival (takeoff) scenarios, which are briefly discussed in the upcoming sections.

A. Parking Scenario

The parking scenario is applied when the aircraft is on the ground and is traveling at a very slow speed. The delay power spectra is based on recommendations for urban (nonhilly) areas in [9].

In this scenario, the line of sight is presumed to be blocked, which results in a Rayleigh fading model. This is actually the worst case assumption. However, it models the channel that can exist when there is not a direct line of sight between the ground station and all areas where aircrafts may be taxiing or parking.

Due to the fact that the aircraft is parked at the terminal or traveling at a very low speed, the vehicle speed is very low (typically $v = 0, \cdots 5.5$ m/s). Thus, the Doppler has minor influence and in this study, it has been neglected.

The maximum delay: $\tau_{\max} = 7\mu s$. The distribution of the delays is exponentially decreasing with a slope of $\tau_{slope} = 1\mu s$.

B. Arrival Scenario

The arrival and takeoff scenarios can be applied when the aircraft is engaged in ground-air communications, has already left its cruising speed and altitude, and is about to land (and vice versa). During this time, it is assumed that the line of sight path is present during the arrival when the vehicle is still airborne. The scattered path components that my arise from interactions with the buildings at the ground station may be modeled as a Rayleigh process. The result is a Ricean channel model, wherein the Ricean factor is set equal to $K_{Rice} = 15$ dB, which presumes a very strong line of sight component.

Since the aircraft is still some distance away from the landing area, excess delays up to $\tau_{\max} = 7\mu s$ are assumed, as in [10].

VI. NUMERICAL RESULTS AND DISCUSSION

In this section, we present simulation results to show the coded bit error rate performance in various environments. In all of the reported cases, a PCM-FM waveform is sampled once per symbol interval ($N_s = 1$) to produce a PCM-FM/CPM-OFDM modulation. In this case (and commensurate with the definition of PCM-FM), we define $L = 2$, $h = 7/10$ and
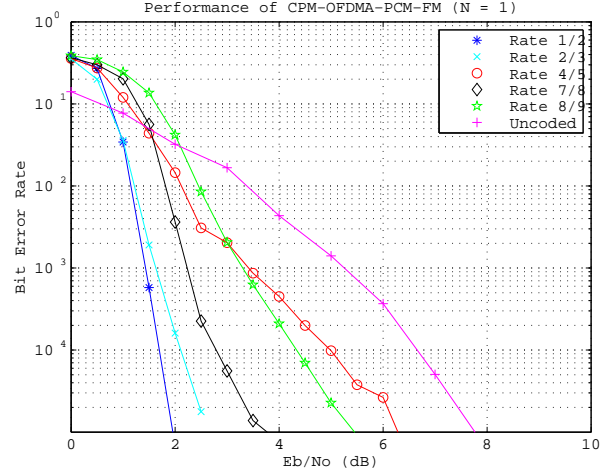

Fig. 2. Coded and uncoded bit error rate performance for CPM-OFDMA-PCM/FM ($N = 1$).

$M = 2$. The number of iterations of the SISO modules is set equal to twenty, and in all cases the simulation halts once 50 packet errors have been detected, where one packet contains $J = 1024$ (or $J = 1022$ information bits), depending on the coding rate.

A. Coded Bit Error Rate Performance in the AWGN Channel

We first present the coded bit error rate performance for PCM-FM/CPM-OFDM in the AWGN channel.

Fig. (2) illustrates the results. As indicated, the performance of uncoded conventional PCM/FM achieves a BER of 10^{-5} at the highest signal-to-noise ratio (7.8 dB in this case). Clearly, the rate $1/2$ code provides excellent bit error rate performance, achieving the same target BER at a signal-to-noise ratio of 2 dB. This represents a 6 dB gain in performance over conventional, uncoded PCM/FM. Even the rate $8/9$ code is able to achieves a 2 dB gain over uncoded PCM/FM, thus exhibiting the advantage of using high rate coding with CPM-OFDMA over the AWGN channel.

B. Coded Bit Error Rate Performance in the Aeronautical Arriving (Take Off) Environment

In this section, we report the performance of coded CPM-OFDMA-PCM/FM in the Aeronautical Arrival channel. Recall that this environment has a strong line of sight component, with some scattering off buildings in the vicinity of the ground station.

TABLE III
NUMBER OF INFORMATION AND CODED BITS

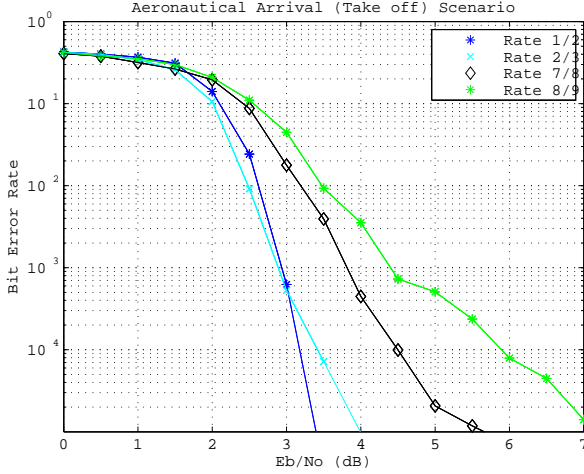| Coding Rate	Information Bits	Coded Bits
1/2	1024	2048
2/3	1024	1536
7/8	1022	1168
8/9	1024	1152

Fig. 3. Coded bit error rate performance for CPM-OFDMA-PCM/FM (N = 1) in the Aeronautical Arrival (Take Off) environment.

Fig. 4. Coded bit error rate performance for CPM-OFDMA-PCM/FM (N = 1) in the Aeronautical Parking channel environment.

Due to the presence of the wideband channel, we have applied the MMSE single-tap frequency domain equalizer to the channel-impaired waveform.

As shown in Fig. (3), we have achieved excellent performance, even for the rate $8/9$ code, which attains a BER of 10^{-5} at an E_b/N_0 of 7 dB. The rate $1/2$ code achieves a BER of 10^{-5} at an E_b/N_0 of 3.2 dB.

C. Coded Bit Error Rate Performance in the Aeronautical Parking Environment

In this section, we present the BER performance when the CPM-OFDMA-PCM-FM signal is passed through a frequency selective fading channel that is representative of the the Aeronautical Parking environment. As mentioned previously, this environment captures a worst case situation, wherein the aircraft is parked and does not have a line of sight path to the ground station. Hence, the channel is marked by Rayleigh fading.

As with the Aeronautical Arriving (Take Off) environment, we have applied MMSE frequency domain equalization to the channel-impaired signal.

The results are provided in Fig. (4), where we illustrate how the rates $1/2$ and $2/3$ codes provide good protection to the CPM-OFDMA-PCM-FM waveform. In summary, the rate $2/3$ code is able to achieve a BER of 10^{-5} at an E_b/N_0 of 9.2 dB, while the rate $1/2$ code achieves the same BER at an E_b/N_0 of 6.2 dB. Even in this severe fading channel, the coding is able to reduce the impact of the channel using a low complexity equalizer strategy.
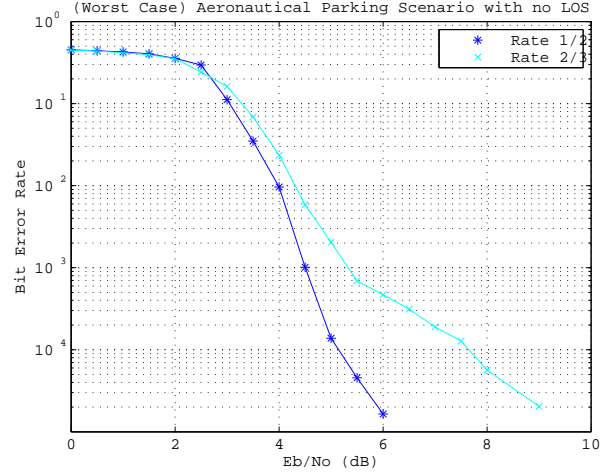
VII. CONCLUSION

In this paper, we have presented a spectrally efficient CPM-OFDM modulation, which takes just one sample per symbol interval of a PCM-FM waveform and uses the resulting stream of signal samples as the input to an OFDM modulator. We have demonstrated that this scheme can also be used as the inner code in a serially concatenated convolutionally encoded scheme that can be used in frequency selective fading channel environments. As demonstrated, a 6 dB gain in receiver performance can be achieved in the AWGN channel by using rate $1/2$ code over uncoded PCM-FM. Furthermore, a 2 dB gain can still be achieved in the same enviroment using a rate $8/9$ code. We have also demonstrated the use of low complexity frequency domain equalization techniques at the receiver. In particular, in the frequency selective fading environment, the serially concatenated convolutionally encoded PCM-FM/CPM-OFDM scheme provides very good immunity to the impairments that are introduced to the transmitted signal.

REFERENCES

[1] J. B. Anderson, T. Aulin, and C.-E. Sundberg, *Digital Phase Modulation*. New York: Plenum Press, 1986.
[2] T. Hill, "An enhanced, constant envelope, interoperable shaped offset QPSK (SOQPSK) for improved spectral efficiency," in *Proc. Int. Telemetering Conf.*, (San Diego, CA), Oct. 2000.
[3] E. Law and K. Feher, "FQPSK versus PCM/FM for aeronautical telemetry applications; spectral occupancy and bit error probability comparisons," in *Proc. Int. Telemetering Conf.*, (Las Vegas, NV), pp. 489–496, Oct. 1997.

[4] Range Commanders Council Telemetry Group, Range Commanders Council, White Sands Missile Range, New Mexico, *IRIG Standard 106-04: Telemetry Standards*, 2004. (Available on-line at http://www.ntia.doc.gov/osmhome/106.pdf).

[5] S. Thompson, A. Ahmed, J. Proakis, J. Zeidler, and M. Geile, "Constant envelope OFDM," *IEEE Trans. Commun.*, vol. 56, pp. 1300–1312, Aug. 2008.

[6] J. Tan and G. Stüber, "Constant envelope multi-carrier modulation," in *IEEE MILCOM*, Oct. 2002.

[7] S. Lin and D. Costello, *Error Control Control*. New York: Prentice Halll, 2004.

[8] E. Haas, "Aeronautical channel modeling," *IEEE Trans.Veh. Tech.*, vol. 51, pp. 254–264, March 2002.

[9] M. Failli, "Digital land mobile radio systems," Sept. 1988. COST 207 Final Rep.

[10] G. Dyer and T. Gilbert, "Channel sounding measurements in the vhf a/g radio communications channel," Apr. 1997. AMCP doc. AMCP/WG-D/7-WP/27.

[11] P. Moqvist and T. Aulin, "Trellis termination in CPM," *Elec. Letters*, vol. 36, pp. 1940–1941, Nov. 2000.

[12] G. M. S. Benedetto, D. Divsalar and F. Pollara, "A soft-input soft-output app module for iterative decoding of concatenated codes," *IEEE Comm. Lett.*, vol. 1, pp. 22–24, Jan. 1997.